NANO LETTERS

2005
Vol. 5, No. 10
2034−2038

Localized Surface Plasmon Resonance Spectroscopy of Single Silver Nanocubes

Leif J. Sherry, Shih-Hui Chang, George C. Schatz,* and Richard P. Van Duyne*

Chemistry Department, Northwestern University, 2145 Sheridan Road, Evanston, Illinois 60208-3113

Benjamin J. Wiley and Younan Xia

Department of Chemistry, University of Washington, Seattle, Washington 98195

Received August 10, 2005

ABSTRACT

In this work, we use dark-field microscopy to observe a new plasmon resonance effect for a single silver nanocube in which the plasmon line shape has two distinct peaks when the particles are located on a glass substrate. The dependence of the resonance on nanocube size and shape is characterized, and it is found that the bluer peak has a higher figure of merit for chemical sensing applications than that for other particle shapes that have been studied previously. Comparison of the measured results with finite difference time domain (FDTD) electrodynamics calculations enables us to confirm the accuracy of our spectral assignments.

The optical properties of metal nanoparticles have been the subject of intensive research efforts because of their applications in research areas such as surface-enhanced spectroscopies,[1−4] second harmonic generation,[5−8] and chemical/biological sensing.[9−14] Recent advances in both lithographic and wet chemical techniques have made it possible to synthesize a wide range of particle sizes and geometries, which exhibit widely varying optical responses.[15−18] These responses, though spectroscopically diverse, are due to a single phenomenon known as the localized surface plasmon resonance (LSPR), which is a result of collective oscillations of a nanoparticle's conduction band electrons.[1] Mie theory, which was first described in 1908, can be used to understand LSPRs for a sphere.[19] For more complex geometries (e.g., cylinders, triangular prisms, cubes, etc.), however, one must employ more advanced electrodynamic numerical methods in order to correctly describe metal nanoparticle optical properties. Previous studies have shown the LSPR to be intimately related to a nanoparticle's size, shape, composition, and dielectric environment.[1,9,10,16,20−24] In fact, these studies have shown the LSPR resonance position to be highly tunable across a wide spectroscopic range by only varying the size of the nanoparticle,[22] and that LSPR resonances are due not only to dipolar excitations but also to higher-order multipolar excitations for certain nanoparticle structures.[16]

Much of the recent attention concerning metal nanoparticles has been concerned with their use as small-volume, ultrasensitive sensors.[9−14] These studies exploit the environmental sensitivity of a nanoparticle's LSPR spectrum by exposing a nanoparticle to solvents of varying refractive indexes and by modifying a nanoparticle's surface with a self-assembled monolayer (SAM) of small-molecule adsorbates. Intrinsic to this type of study is the need to immobilize the nanoparticles on a substrate, particularly if one is interested in working with single nanoparticles. Van Duyne, Schatz, and co-workers have investigated the effect of dielectric substrates on the LSPR extinction of metallic nanoparticle arrays.[25] Kreibig and co-workers have compared the effects of dielectric, semiconductor, and metallic substrates on nanoparticle optical properties with a nanoparticle positioned at different heights relative to the substrate surface.[26] A conclusion from both of these investigations is that plasmon resonances are red-shifted (relative to the particles in a vacuum) because of interactions with the substrate, with the amount of the red-shift being determined by the dielectric constant of the substrate and by the distance between the particle and substrate. If the particle is in contact with the substrate, then the size of the red-shift depends on the fractional area of the particle which is in contact with the substrate. While these studies are of high quality and correctly predict the influence of the substrate on the

* Corresponding authors: Richard P. Van Duyne, vanduyne@chem.northwestern.edu, Telephone (847) 491-3516, Fax (847) 491-7713 and George C. Schatz, schatz@chem.northwestern.edu, Telephone (847) 491-5657; Fax (847) 491-7713.

10.1021/nl0515753 CCC: $30.25
Published on Web 08/27/2005

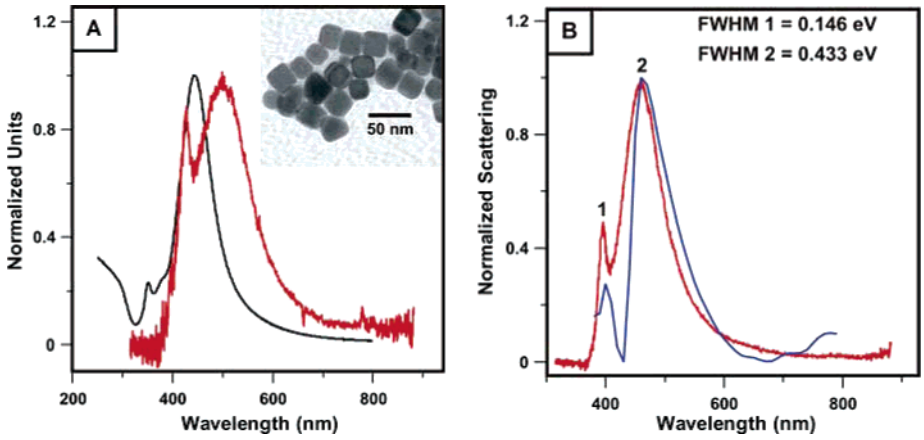

Figure 1. Comparison of the LSPR spectra of (A) nanocube ensemble extinction (black) and single nanocube dark-field scattering (red) in H_2O environment and (B) single nanocube dark-field scattering (red) and FDTD theory (blue) in a nitrogen environment. The calculation in part B was performed for a 36-nm nanocube on a glass substrate.

resonance spectral location, they are performed on nanoparticles of limited geometrical diversity (i.e., truncated tetrahedrons having a maximum height of 50 nm and small (<10 nm) spheres, respectively).

In the current study, we investigate the influence of a dielectric substrate on the LSPR spectrum of a nonspherical silver nanoparticle, specifically a nanocube, and show how the nanocube's LSPR spectrum is uniquely altered by the presence of such a substrate. In contrast to the earlier work, this study involves measurements on single particles (using dark-field microscopy), rather than an ensemble, thereby removing the effect of averaging and enabling us to observe previously unsuspected details of the effects of substrate interactions. In particular, we find that there are *two* plasmon resonance peaks when a silver cube interacts with a glass substrate, one of which is red-shifted relative to the bulk spectrum (where only a single peak is observed) and the other being blue-shifted and considerably narrower. The blue-shifted resonance was not anticipated on the basis of earlier work, but we use finite difference time domain electrodynamics calculations to confirm that this is the expected result for this nanoparticle geometry. In addition, we show that the blue-shifted resonance shows promise for applications in plasmonic sensing due to its narrow width. While most plasmonic sensing studies to date have focused on creating systems that maximize the absolute shift of the plasmon peak due to molecular absorption to nanoparticles,[10−14] recent interest in the creation and utilization of narrow plasmons for sensing applications has increased,[27−29] as optimum sensitivity sometimes occurs because of plasmon narrowing rather than index shifting. To study this issue, we define and evaluate a figure of merit (FOM) for sensing and compare values for a variety of nanoparticle structures.

Cubic silver nanoparticles were prepared by the Xia group using the polyol synthetic technique as described elsewhere.[15] These cubes have a 30-nm edge length on average. To explore the substrate−nanoparticle interaction, the nanocubes were immobilized randomly on a no. 1 glass coverslip by drop-coating approximately 1 μL of nanoparticle solution and allowing the solvent to evaporate. The coverslip was then placed in a custom-made flow cell where the nanoparticles could be exposed to various dielectric environments. Prior to acquiring data, the nanocubes were rinsed multiple times with methanol in order to ensure surface equilibrium and geometrical stability.

Single-nanoparticle optical data were obtained by use of resonant Raleigh dark-field optical microscopy. This technique utilizes an inverted microscope (Eclipse TE300, Nikon Instruments) equipped with a dark-field condenser (NA = 0.95) for nanoparticle illumination and a 100× variable aperture oil immersion objective (NA = 0.5−1.3) for subsequent collection of a nanoparticle's scattered light. In this technique, a solid circular annulus located in the light condenser blocks a portion of the incoming light so as to create a hollow light cone. This light cone focuses at an angle such that no light from the source is directly collected by the objective. This creates an image with an extremely low background, thus enabling high signal-to-noise spectra of single nanoparticles. As such, the single nanoparticle LSPR spectra acquired in this study are spectra purely of Rayleigh scattered light, and the scattering angle is roughly 90 ± 30°. The apparatus for these measurements is coupled to an imaging spectrograph (SpectroPro 300i, Roper Scientific) and a CCD detector (Spec-10:400B, Roper Scientific). We also generated results for ensembles of nanoparticles in solution using conventional UV−vis transmission spectroscopy. These experiments measure the extinction spectrum, which is the sum of absorption and scattering.

FDTD results were generated using a previously described method.[30] These results describe the behavior of particles in solution and particles on glass, with structural parameters taken to match the experiments as closely as possible. The silver dielectric function was represented using a Drude model, with parameters chosen to match experiments for wavelengths in the 350−600 nm range, similar to the D2 parameter in ref 31. The index of refraction of the glass is taken to be 1.5. The incident wave is launched in a box around the nanoparticle to simulate a plane wave propagating into an infinite half-space filled with glass in the total-field scattered-field formulation.[32]

Figure 1 compares Rayleigh scattering results for a single nanocube on a glass substrate. Figure 1A compares a single

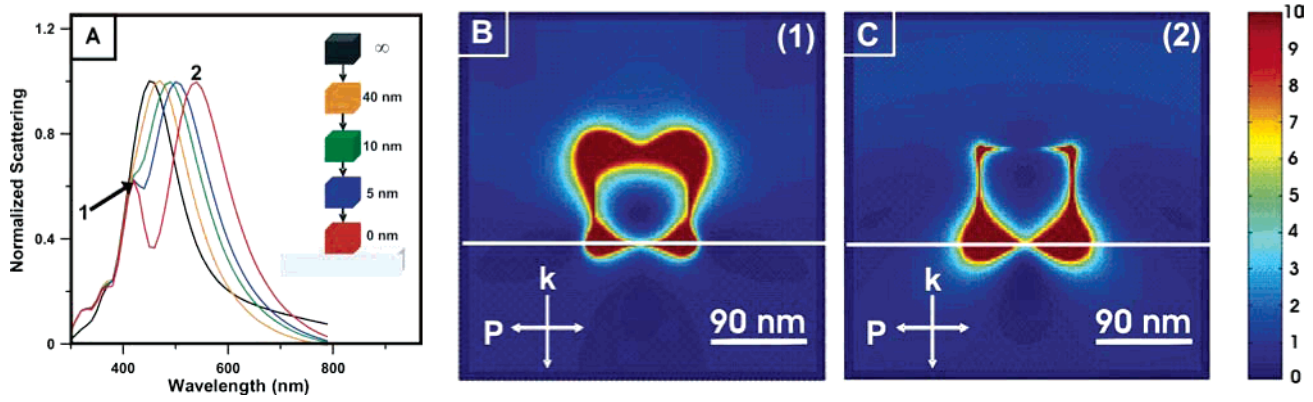

Figure 2. FDTD theory showing (A) the emergence of a second peak as a single nanocube (90-nm diameter) approaches a dielectric substrate, and (B,C) the field intensities for peaks 1 and 2 of the nanocube in contact with the substrate (the white line in the field pattern images represent the substrate).

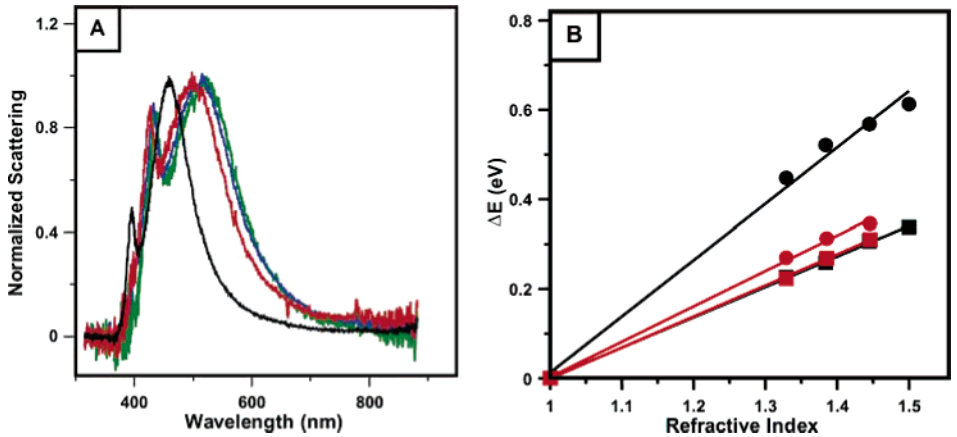

Figure 3. Refractive index sensitivity of single silver nanocubes: (A) single nanocube dark-field scattering spectra in four different dielectric environments (refractive indexes = 1.000 297, 1.329, 1.3854, 1.4458), (B) theoretical (black) and experimental (red) linear regression fits of the relative energy shift for each nanocube peak (circles = peak one; squares = peak two) in the various dielectric environments.

nanocube in water with extinction results for an ensemble of particles in water, and Figure 1B compares a single nanocube experiment in dry nitrogen with an FDTD scattering calculation for a 36-nm edge length nanocube in dry nitrogen. Figure 1A shows that the solution spectra of the cubes has a strong dipole plasmon resonance at 444 nm, while the single nanoparticle spectrum has two peaks, one blue-shifted (peak 1) and one red-shifted (peak 2) from the solution spectrum. The red-shifted peak is consistent with what was found in past studies of other nanoparticle structures,[25] but the blue-shifted peak has not been seen previously,[10,14,22−26] and we note that this peak is quite a bit narrower than the red-shifted peak. The solution spectrum also shows a weak second peak at 351 nm. Our theoretical analysis shows, however, that this peak is not derived from the nanocubes. Hence, we assume that it arises from other particles present in small abundance.

Figure 1B shows that the calculated and measured scattering spectrum for a single particle on a surface match quite well, thereby confirming that the presence of two plasmon resonances when the particle is on the surface is consistent with electrodynamics for the assumed particle structure. To understand the physical origin of these peaks, we show in Figure 2 the near-field behavior associated with the FDTD result for peaks 1 and 2, this time for a larger cube (90 nm), as well as a series of scattering spectra that were generated by moving the cube toward the surface. These spectra show that the dipole mode associated with the solution spectrum shifts into a broad peak at 550 nm when the particle gets within a few nanometers of the surface. In addition, a blue peak appears at 430 nm that becomes more distinct as the particle approaches the surface. Figure 2B,C shows that peak 1 is associated with large fields away from the surface, while peak 2 is associated with large fields toward the surface. This phenomenon shows up clearly with the 90-nm nanocube, and it also occurs for a 30-nm cube but not until it is almost in contact with the glass substrate. Calculations for a cube in water (not shown) also lead to plasmon line shapes with two peaks, as a homogeneous dielectric environment also results in multimodal resonances. The spatial separation in near-field response seen in Figure 2 only occurs for nanoparticles on a substrate.

To further understand these results, we have examined the dependence of the peak wavelengths on the refractive index of solvent above the nanoparticles. Figure 3 presents both experimental (Figure 3A,B) and theoretical (Figure 3B) results, and we see a linear dependence of wavelength on refractive index that is similar to what has been seen earlier

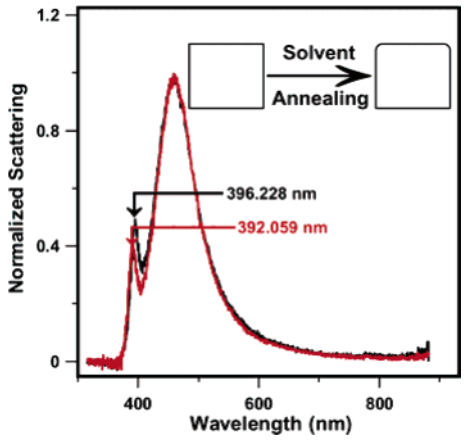

Figure 4. Dark-field LSPR scattering spectra for a single nanocube before (black) and after (red) solvent annealing with methanol.

in studies of other nanoparticle structures.[9,10,14,22] Linear regression yields experimental slopes of 0.792 eV RIU^{-1} (peak 1) and 0.695 eV RIU^{-1} (peak 2; RIU = refractive index unit), which are smaller values than have been seen in studies of triangular nanoparticles.[10]

Intuition tells us that the redder resonance (peak 2) should be less dependent on changes in the bulk dielectric environment than peak 1, since this resonance mostly involves polarization excited at the surface. Indeed, one can see in both theory and experiment that, as the refractive index of the dielectric medium increases, peak 1 shifts more readily to higher energy than peak 2. Although both theory and experiment show the same trend (Figure 3B), the experimental slope for peak 1 is well below the theoretical value, while theory and experiment have almost exactly the same slopes for peak 2. To explain this, we hypothesize that upon exposure to the initial methanol rinsing the nanocubes suffer nonsymmetrical annealing in which the nanocube corners not in contact with the glass substrate are rounded, while the corners in contact with the substrate are left virtually unchanged. This causes the nanocube corners not in contact with the glass substrate to have a larger radius of curvature, and on the basis of our earlier work, this means a lessened sensitivity to changes in dielectric environment.[10,33]

To test this hypothesis, we acquired two dark-field LSPR scattering spectra in dry nitrogen: one before methanol rinsing and one after. If the methanol rinsing causes inhomogeneous solvent annealing of the nanocubes, the scattering spectra should reflect this with inhomogeneous blue-shifts in the resonance peaks due to overall reduction in the nanocube's size.[33] Indeed, Figure 4 shows precisely this type of behavior. Peak 1 experiences a 4.17-nm blue-shift, while peak 2 remains unchanged. To substantiate this result, we performed a theoretical study of nanocubes with rounded corners using the FDTD method. The theory shows that, if the nanocube's top corners are annealed, peak 1 blue-shifts while peak 2 remains unchanged (not shown), and if the bottom corners are annealed, peak 2 blue-shifts. The experimental results, when compared to theory, are consistent with a ~2-nm annealing of the top corners leading to peak 1's observed 4.17-nm blue-shift. This theory result also confirms that peak 1 is the resonant mode associated with the top corners of the nanocube and peak 2 is the resonant mode associated with the bottom corners.

To more thoroughly understand the geometric dependence of this phenomenon, we conducted theoretical studies on how shape and size influence a single nanoparticle's LSPR scattering spectrum. To model the substrate effect for particles with different shapes, we conducted FDTD calculations for spherical particles at progressively smaller distances above a glass substrate as done in Figure 2 for the nanocubes. In these studies, we found only one plasmon resonance as the nanoparticle approaches and comes into contact with the substrate. If, however, the nanospheres are partially submerged into the substrate, two peaks appear in the line shape. This result is consistent with the location of hot spots for the different nanoparticle structures.[34] If the near-field intensity is very high both above and below the particle when it is in contact with the substrate, as is shown in Figure 2 for a cubic particle, then two peaks can result. For spheres, however, the highest intensities (for polarization parallel to the surface) are near the equatorial regions of the sphere. Hence, the plasmon resonance is controlled by the medium above the substrate when the sphere touches the surface. Only when the nanosphere is submerged in the surface is it possible to generate two peaks.

The size, or thickness, of the nanocube also proved to be critical in creating the sharp resonance in Figure 1. For nanocubes smaller than the skin depth (~20 nm), the two resonances merge. In this situation, the asymmetric dielectric environment is averaged in determining the overall response.

Now, we consider the possibility of exploiting the extreme sharpness of peak 1 (fwhm = 0.146 eV) in chemical sensing applications. Although peak 1 proved to be less sensitive to changes in its dielectric environment than previous studies have shown for other nanoparticle geometries,[10] the overall refractive index sensitivity also depends on the fwhm. Hence, we define a "figure of merit" (FOM) in order to directly compare the overall performance of single nanoparticles as chemical sensors

$$\mathrm{FOM} = \frac{m\ (\mathrm{eV\ RIU^{-1}})}{\mathrm{fwhm\ (eV)}} \qquad (1)$$

where m is the linear regression slope for the refractive index dependence. This definition allows nanoparticles to be judged against one another as sensing platforms independent of shape or size. Experiments on triangular nanoprisms synthesized via wet chemical techniques[35] have yielded FOMs averaging ~3. For the nanocube measurement in Figure 1B, we find a FOM of 1.6 for peak 2 and 5.4 for peak 1, the highest value we have obtained so far in isolated nanoparticle applications.

In summary, we report the existence of two plasmon resonances for silver nanocubes interacting with a glass substrate as a new substrate effect in single nanoparticle spectroscopy. This behavior has been found using FDTD theory, and we have observed it experimentally via resonant Raleigh, dark-field optical microscopy. Different dielectric

environmental dependencies are observed for each resonance, with theory and experiment again in reasonable accord. We found that the two peaks are not obtained for spherical shapes, unless the particles are partially embedded in the surface, or for cubes, unless they are thicker than the skin depth. This shows that the plasmon resonance structure of a nanoparticle in contact with a dielectric substrate is shape and size dependent. Cube-shaped particles are ideal for the production of two resonances, as large polarizations are induced on both top and bottom surfaces of the particles, with the bluer of the two resonances having exceptional sensing capabilities due to its extreme sharpness. Current work is underway to explore single nanocubes as chemical sensors. In addition, it may be possible to obtain further experimental observations of the reported substrate effect for a wider range of nanoparticle geometries thanks to recent advances in substrate modification[35] and wet chemical synthetic techniques.[36]

Acknowledgment. This work was supported by the National Science Foundation (EEC-0118025, CHE-0414554) and the Air Force Office of Scientific Research MURI program (F49620-02-1-0381). The authors thank Erin McLellan for the TEM images in Figure 1.

References

(1) Schatz, G. C.; Van Duyne, R. P. In *Handbook of Vibrational Spectroscopy*; Chalmers, J. M., Griffiths, P. R., Eds.; Wiley: New York, 2002; Vol. 1, pp 759−774.
(2) Freeman, R. G.; Grabar, K. C.; Allison, K. J.; Bright, R. M.; Davis, J. A.; Guthrie, A. P.; Hommer, M. B.; Jackson, M. A.; Smith, P. C.; Walter, D. G.; Natan, M. J. *Science* **1995**, *267*, 1629−1632.
(3) Kahl, M.; Voges, E.; Kostrewa, S.; Viets, C.; Hill, W. *Sens. Actuators, B* **1998**, *51*, 285−291.
(4) Haynes, C. L.; Van Duyne, R. P. *J. Phys. Chem. B* **2003**, *107*, 7426−7433.
(5) Hao, E. C.; Schatz, G. C.; Johnson, R. C.; Hupp, J. T. *J. Chem. Phys.* **2002**, *117*, 5963−5966.
(6) Podlipensky, A.; Lange, J.; Seifert, G.; Graener, H.; Cravetchi, I. *Opt. Lett.* **2003**, *28*, 716−718.
(7) Chen, C. K.; Heinz, T. F.; Richard, D.; Shen, Y. R. *Phys. Rev. B* **1983**, *27*, 1965−1979.
(8) Moran, A. M.; Sung, J.; Hicks, E. M.; Van Duyne, R. P.; Spears, K. G. *J. Phys. Chem. B* **2005**, *109*, 4501−4506.
(9) Haes, A. J.; Zou, S.; Schatz, G. C.; Van Duyne, R. P. *J. Phys. Chem. B* **2004**, *108*, 6961−6968.
(10) McFarland, A. D.; Van Duyne, R. P. *Nano Lett.* **2003**, *3*, 1057−1062.
(11) Haes, A. J.; Van Duyne, R. P. *J. Am. Chem. Soc.* **2002**, *124*, 10596−10604.
(12) Haes, A. J.; Hall, W. P.; Chang, L.; Klein, W. L.; Van Duyne, R. P. *Nano Lett.* **2004**, *4*, 1029−1034.
(13) Nam, J. M.; Thaxton, C. S.; Mirkin, C. A. *Science* **2003**, *301*, 1884−1886.
(14) Mock, J. J.; Smith, D. R.; Schultz, S. *Nano Lett.* **2003**, *3*, 485−491.
(15) Wiley, B.; Sun, Y.; Mayers, B.; Xia, Y. *Chem.—Eur. J.* **2005** *11*, 454−463.
(16) Jin, R.; YunWei, C.; Mirkin, C. A.; Kelly, K. L.; Schatz, G. C.; Zheng, J. G. *Science* **2001**, *294*, 1901−1903.
(17) Sau, T. K.; Murphy, C. J. *Langmuir* **2004**, *20*, 6414−6420.
(18) Chen, J.; Saeki, F.; Wiley: B. J.; Cang, H.; Cobb, M. J.; Li, Z. Y.; Au, L.; Zhang, H.; Kimmey, M. B.; Li, X.; Xia, Y. *Nano Lett.* **2005**, *5*, 473−477.
(19) Mie, G. *Ann. Phys.* **1908**, *25*, 377.
(20) Mock, J. J.; Barbic, M.; Smith, D. R.; Schultz, D. A.; Schultz, S. *J. Chem. Phys.* **2002**, *116*, 6755−6759.
(21) Haynes, C. L.; Van Duyne, R. P. *J. Phys. Chem. B* **2001**, *105*, 5599−5611.
(22) Jensen, T. R.; Malinsky, M. D.; Haynes, C. L.; Van Duyne, R. P. *J. Phys. Chem. B* **2000**, *104*, 10549−10556.
(23) Sönnichsen, C.; Geier, S.; Hecker, N. E.; von Plessen, G.; Feldmann, J.; Ditlbacher, H.; Lamprecht, B.; Krenn, J. R.; Aussenegg, F. R.; Chan, V. Z.-H.; Spatz, J. P.; Möller, M. *Appl. Phys. Lett.* **2000**, *77*, 2949−2951.
(24) Klar, T.; Perner, M.; Grosse, S.; von Plessen, G.; Spirkl, W.; Feldmann, J. *Phys. Rev. Lett.* **1998**, *80*, 4249−4252.
(25) Malinsky, M. D.; Kelly, K. L.; Schatz, G. C.; Van Duyne, R. P. *J. Phys. Chem. B* **2001**, *105*, 2343−2350.
(26) Pinchuk, A.; Hilger, A.; von Plessen, G. Kreibig, U. *Nanotechnology* **2004**, *15*, 1890−1896.
(27) Zou, S.; Janel, N.; Schatz, G. C. *J. Chem. Phys.* **2004**, *120*, 10871−10875.
(28) Zou, S.; Schatz, G. C. *J. Chem. Phys.* **2004**, *121*, 12606−12612.
(29) Hicks, E. M.; Zou, S.; Gunnarsson, L.; Rindzevicius, T.; Kasemo, B.; Käll, M.; Schatz, G. C.; Spears, K. G.; Van Duyne, R. P. *Nano Lett.* **2005**, *5*, 1065−1070.
(30) Chang, S.-H.; Gray, S. K.; Schatz, G. C. *Opt. Express* **2005**, *13*, 3150−3165.
(31) Gray, S. K.; Kupka T. *Phys. Rev. B* **2003**, *68*, 045415(1−11).
(32) Taflove, A.; Hagness, S. C. *Computational Electrodynamics: The Finite-difference Time-Domain Method*, 2nd ed.; Artech House: Boston, 2000.
(33) Kelly, K. L.; Coronado, E.; Zhao, L. L.; Schatz, G. C. *J. Phys. Chem. B* **2003**, *107*, 668−677.
(34) Hao. E.; Schatz, G. C. *J. Chem. Phys.* **2004**, *120*, 357−366.
(35) Whitney, A. V.; Myers, B. D.; Van Duyne, R. P. *Nano Lett.* **2004**, *4*, 1507−1511.
(36) Métraux, G. S.; Mirkin, C. A. *Adv. Mater.* **2005**, *17*, 412−415.

NL0515753